

# Drug Delivery Systems-Based Dendrimers and Polymer Micelles for Nuclear Diagnosis and Therapy

Liliana Aranda-Lara, Blanca Eli Ocampo García, Keila Isaac-Olivé, Guillermina Ferro-Flores, Laura Meléndez-Alafort, and Enrique Morales-Avila\*

Polymeric nanoparticles encompass micelles and dendrimers. They are used for improving or controlling the action of the loaded therapy or imaging agent, including radionuclides. Some radionuclides possess properties appropriate for simultaneous imaging and therapy of a disease and are therefore called theranostic. The diversity in core materials and surface modification, as well as radiolabeling strategies, offers multiples possibilities for preparing polymeric nanoparticles using radionuclides. The present review describes different strategies in the preparation of such nanoparticles and their applications in nuclear nanomedicine.

## 1. Introduction

### 1.1. Pharmaceutical Nanotechnology and Nanomedicine

The understanding of matter's behavior at nanometric scales and its advantages has influenced the exponential development in pharmaceutical medicine and translational clinical research. Pharmaceutical nanotechnology and nanomedicine provide alternatives to build biologically-active molecules formulated as nanoparticles, with different sizes, shapes, and composition, using a rational design with physicochemical properties and biological functions for diagnosis and treatment of several diseases.<sup>[1–5]</sup>

Nanometric delivery systems, such as polymeric nanoparticles, have been developed for improving or controlling the pharmaceutical action of loaded drug or imaging agent, through the

selective accumulation in the pathological compartment, with minimal loss due to metabolism, clearance, or unspecific distribution to prevent side effects to healthy tissues.<sup>[6–8]</sup> Nevertheless, the FDA approval of nanotechnology-based treatments and its clinical translation remains relatively low.

The physicochemical properties and biological functions of nanoparticles are as complex as the molecule designed, due to the great availability of biomaterials and bioactive molecules, drug-loading methods, along with different pharmaceutical manufacturing processes. Therefore, the possibilities for building pharmaceutical nanomaterials for diagnostic and therapeutic applications are unlimited (Figure 1). Likewise, the biological responses and physiological functions become complex as the building possibilities become endless.<sup>[8–10]</sup>

### 1.2. Polymeric Nanoparticles in Nanomedicine

Polymeric controlled-release and drug-targeting nanoparticle systems, such as dendrimers and polymeric micelles, are globular nanostructures prepared with amphiphilic copolymers and lipophilic cores. These polymeric systems represent an alternative to traditional formulations, with the advantage of improving the transport into the target cell and the pharmacokinetics of cytotoxic molecules getting similar or better efficacy compared to free drug, but with less or no toxicity.<sup>[11,12]</sup>


Dendrimers are hyperbranched polymers of homogeneous composition with a compact globular structure characterized by layers (called generations or focal points) emanating from the central nucleus to the surface by modular construction. The core can be composed of polymers as polypropylene imine (PPI), poly(amidoamine) (PAMAM), polyethylene glycol (PEG), and others, although the most used is PAMAM. The functional groups of the surface define the anionic, cationic, or neutral character of the dendrimer. Its properties are similar to those of biomolecules. Dendrimers represent a class of polymers with unique molecular architectures characterized by a hyperbranched and well-defined structure and homogeneous composition, resulting in a high degree of molecular uniformity, highly controllable size, and modifiable surface properties. They present low polydispersity and high colloidal stability, which make them attractive materials for the development of nanomedicines. Pharmacokinetic properties are the most

L. Aranda-Lara, K. Isaac-Olivé  
Facultad de Medicina  
Universidad Autónoma del Estado de México  
Paseo Tollocan S/N, Toluca, Estado de México 50180, Mexico

B. E. García, G. Ferro-Flores  
Instituto Nacional de Investigaciones Nucleares  
Carretera México-Toluca S/N, Ocoyoacac, Estado de México 52750, Mexico

L. Meléndez-Alafort  
Veneto Institute of Oncology IOV-IRCCS  
Via Gattamelata 64, Padova 35128, Italy

E. Morales-Avila  
Facultad de Química  
Universidad Autónoma del Estado de México  
Paseo Tollocan S/N, Toluca, Estado de México 50180, Mexico  
E-mail: emoralesav@uaemex.mx; enrimorafm@yahoo.com.mx

 The ORCID identification number(s) for the author(s) of this article can be found under <https://doi.org/10.1002/mabi.202000362>.

DOI: 10.1002/mabi.202000362

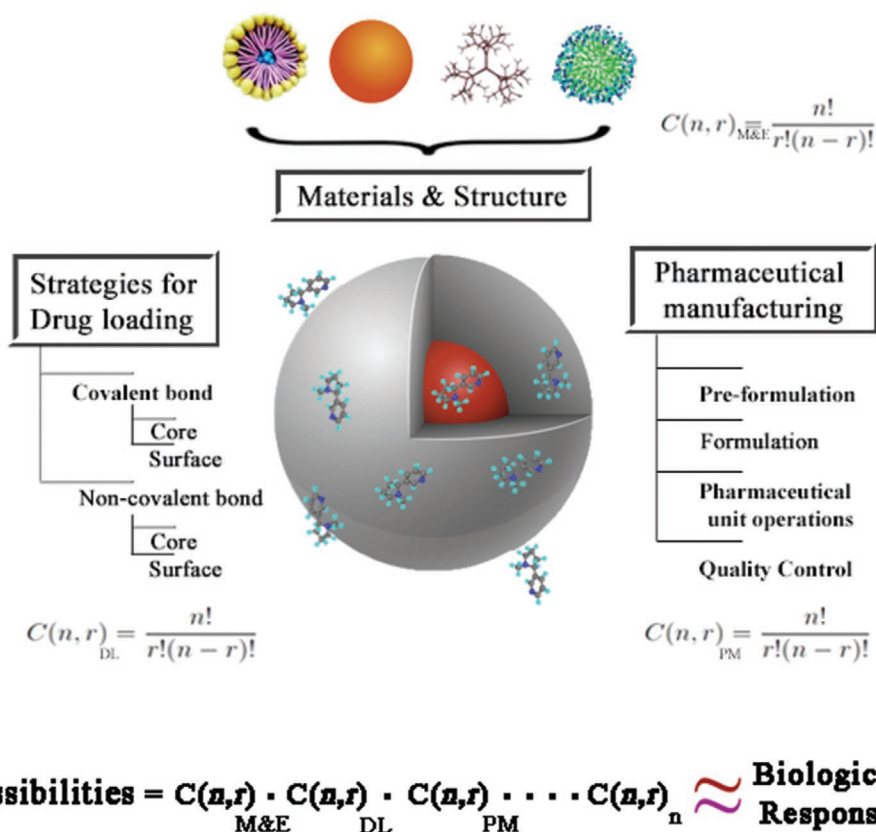


Figure 1. Possibilities for building pharmaceutical nanomaterials.

significant aspects that need to be considered for the successful biomedical application of dendrimers.<sup>[13,14]</sup>

Depending on the nature of the nanoparticle core, hydrophobic, or hydrophilic drugs can be transported.<sup>[7,9]</sup> The organic nature and the chemical resilience of the nanoparticle surface are suitable for exploring the multivalent and multimeric effect by conjugation of specific ligands, for increased retention at the target site and uptake by the target cells. Furthermore, in order to improve smart drug delivery characteristics, surface modifications are used to make nanocarriers sensitive to different stimuli such as temperature, pH, magnetic fields, ultrasonic waves, light, and feedback-regulated release.<sup>[3,15]</sup>

Polymeric micelles are spherical colloidal particles, thermodynamically formed when the hydrophobic ends of the copolymers that form them intertwine and form a nucleus, while the hydrophilic ends are exposed on the surface, ensuring their solubility.

Preparation of polymeric micelles at a nanometric range can be easily and efficiently achieved using amphiphilic polymers such as lactide-poly (ethylene glycol) (L-PEG), poly(lactide) (PL), and its copolymers poly(lactide-co-glycolide) acid (PLGA). These nanoparticles can be prepared using the single oil-in-water or a double water-in-oil-in-water (W/O/W) droplet method, leading to nanoparticle assembly by hydrophobic and hydrophilic effects. Additionally, molecules can be included on the nanoparticle surface or inside the polymer core, depending on its affinity for the environment and for the composition of the nanoparticle.

Two important parameters for polymeric nanoparticle engineering are the drug-loading content and drug-loading efficiency. Drug-loading content is correlated with the mass ratio of drug retained by the nanocarrier. This parameter is determined by the structure and physicochemical properties of the nanocarrier material, which determines the interaction forces and favorable thermodynamic behavior. Drug-loading efficiency reflects the ratio between the drugs retained by the nanocarrier, related to the initial amount of drug. This parameter is determined by the drug-loading mechanism, including the mass of drug in feed, chemical conjugation through covalent and coordination bonding or non-covalent bonding (electrostatic complex formation, hydrophobic interaction, and hydrogen bonding), and other experimental conditions.<sup>[16]</sup> However, nanocarrier engineering and the understanding of the biological effects is a pending and difficult subject to elucidate. Recent investigations show that different self-assembly and drug-loading methods affect the biological activities (cytotoxic effects, specific recognition, non-specific recognition, etc.).<sup>[17]</sup>

One field of application of polymeric nanoparticles is nuclear medicine. This is a highly multidisciplinary specialty that uses non-invasive procedures based on radiopharmaceuticals to study physiological processes useful in the diagnosis, monitoring, and treatment of diseases.<sup>[18]</sup> A nano-radiopharmaceutical is defined as a formulation that contains a radionuclide attached to a nanometer-sized molecule used on therapeutic or diagnostic procedures. Depending on the application of the

polymeric nanoparticle, there are different radiolabeling strategies such as complex formation through chelating agents, direct incorporation of the radionuclide (by electrostatic interactions, adsorption phenomenon, or covalent bonding), or confinement strategies (entrapment or encapsulation). The advantages of these strategies will depend on the physiological environment and radiochemical parameters such as radiolabeling efficiency, specific activity, and radiochemical purity. In this work, a general outline of the radiolabeling of polymeric nanoparticles for nanomedicine applications is described.

## 2. Polymeric Nanoparticles for Imaging and Therapy

Molecular imaging techniques offer alternatives that provide a spatial-temporal record at a molecular, cellular, or metabolic level. In this sense, numerous approaches have been developed.<sup>[19]</sup> Radiolabeled polymeric nanoparticles are mainly used in imaging techniques due to their accumulation within the tumor through the enhanced permeability and retention effect (EPR) and targeting by taking advantage of a specific ligand-receptor interaction. Radiolabeled nanoparticles with a gamma emitter or a positron emitter allow to know the biodistribution, pharmacokinetic model, and delivery site of the drug carried through single-photon emission computed tomography imaging (SPECT imaging) or positron emission tomography imaging (PET imaging). If the polymeric nanoparticles are labeled with an alpha- or beta-emitting radionuclide, then they are used to impart combined or concomitant therapy (radiotherapy and chemotherapy).

### 2.1. Polymeric Nanoparticles Labeled with Gamma-Emitting Radionuclides (SPECT)

#### 2.1.1. Polymeric Micelles

<sup>99m</sup>Tc and <sup>111</sup>In are the most reported gamma emitters for polymeric micelle labeling. The most common technique for the radiolabeling of micelles with <sup>99m</sup>Tc employs chelating agents such as ethylenediamine tetra(methylene phosphonic acid) (EDTMP), diethylenetriaminepentaacetic acid (DTPA), hydrazinonicotinamide (HYNIC), or citrate complexation (Figure 2a–d). Tricarbonyl direct radiolabeling has also been used, and is based on the [<sup>99m</sup>Tc(CO)<sub>3</sub>(H<sub>2</sub>O)<sub>3</sub>]<sup>+</sup> complex (Figure 2e); this strategy produces high labeling yields (>90%) and high in vitro stability at 24 h post-labeling.<sup>[20–25]</sup>

Biodistribution studies in preclinical phases, using <sup>99m</sup>Tc-polymeric micelles, show a prolonged circulation time suitable for drug delivery purposes, however, in healthy animals, there is a significant accumulation in liver and spleen (and sometimes in bone marrow.<sup>[24,26]</sup> Also, micelles are metabolized through the urinary system, which constitutes their main route of excretion, although biliary excretion has also been evidenced.<sup>[27]</sup> In some cases, an appreciable accumulation in the lungs has been obtained.<sup>[25]</sup> The polymeric nanosystems designed for tumor targeting reach the target tissue without difficulty.<sup>[20,21,23–26]</sup> Table 1 summarizes the characteristics and

radiolabeling methods for polymeric micelles radiolabeled with <sup>99m</sup>Tc and <sup>111</sup>In.

He et al.<sup>[20]</sup> report the synthesis of (PEG-PLGA)-polypeptide K237 (HTMYHHYQHHL) nanoparticles, conjugated to folic acid (FA) and radiolabeled with <sup>99m</sup>Tc, as a drug delivery system for anticancer purposes. K237/FA-PEG-PLGA nanoparticles were prepared using an emulsion method (W/O). <sup>99m</sup>Tc radiolabeling with stannous chloride was superior to 97%. Radiolabeled nanoparticles were stable in serum or saline solution at 24 h. Cell binding and blocking in vitro experiments indicated that the binding of the radiolabeled NPs was mediated by folate receptors (FR) with additional good bioactivity and specificity. Biodistribution analysis showed significant accumulation in the mononuclear phagocyte system. Nanoparticles were metabolized through the urinary system. The scintigraphic images also revealed a high level of radioactivity accumulation in tumor, liver, kidney, and bladder.

<sup>99m</sup>Tc-polymeric nanoparticles, conjugated to proteins, were reported as an alternative for early detection of gastrointestinal stromal tumors. These nanoparticles were prepared by a double emulsion method (W/O/W), using polylactic acid (PLA), polyvinyl alcohol (PVA), and bevacizumab. The direct labeling strategy produced a radiochemical yield superior to 90%. The biodistribution data showed a significant liver and spleen accumulation, with a low uptake by the gastrointestinal tract, brain, and heart. SPECT images of tumor-grafted mice confirm the potential of nanoparticles in the development of molecular diagnosis systems for the early detection of diseases.<sup>[21]</sup>

Similar PLA nanoparticles produced by a double emulsion-solvent evaporation method (W/O/W), stabilized with PVA and functionalized with EDTMP, were reported. <sup>99m</sup>Tc radiolabeling was carried out (Figure 2a) with an efficiency superior to 90%. Biodistribution and SPECT studies showed a renal clearance with a significant accumulation in the liver and spleen; however, radiolabeled nanoparticles showed a high affinity for bone, converting the system into a possible drug delivery vehicle of EDTMP, for future applications in the treatment of bone cancer.<sup>[22]</sup>

Due to their loading capacity, polymeric micelles have been widely studied as drug delivery systems. These globular nanostructures are commonly prepared by amphiphilic copolymers, predominantly with lipophilic cores. Oda et al.<sup>[23]</sup> report the construction of polymeric micelles from 1,2-distearoyl-sn-glycero-3-phosphoethanolamine-*N*-[methoxy(polyethyleneglycol)-2000] (DSPE-mPEG<sub>2000</sub>-NH<sub>2</sub>), which was modified covalently with DTPA via amide formation, by an opening cyclic anhydride reaction. Micelles were radiolabeled with <sup>99m</sup>Tc, obtaining a radiochemical yield near 93.8%, with high in vivo stability for 8 h. Biodistribution studies showed a significantly high uptake in kidney, liver, and spleen as elimination routes; no significant uptake in the stomach or thyroid was observed. The tumor-graft model showed a significant tumor uptake with regard to muscle and normal tissues, indicating that the system might be a suitable platform for drug delivery, combined with alternative radio-diagnostic possibilities.

Poliak et al. report the preparation of <sup>99m</sup>Tc-labeled, folate-targeted, self-assembled polyelectrolyte nanoparticles (75–200 nm), formed from chitosan and poly- $\gamma$ -glutamic acid ( $\gamma$ -PGA), as a new potential SPECT imaging agent for the early

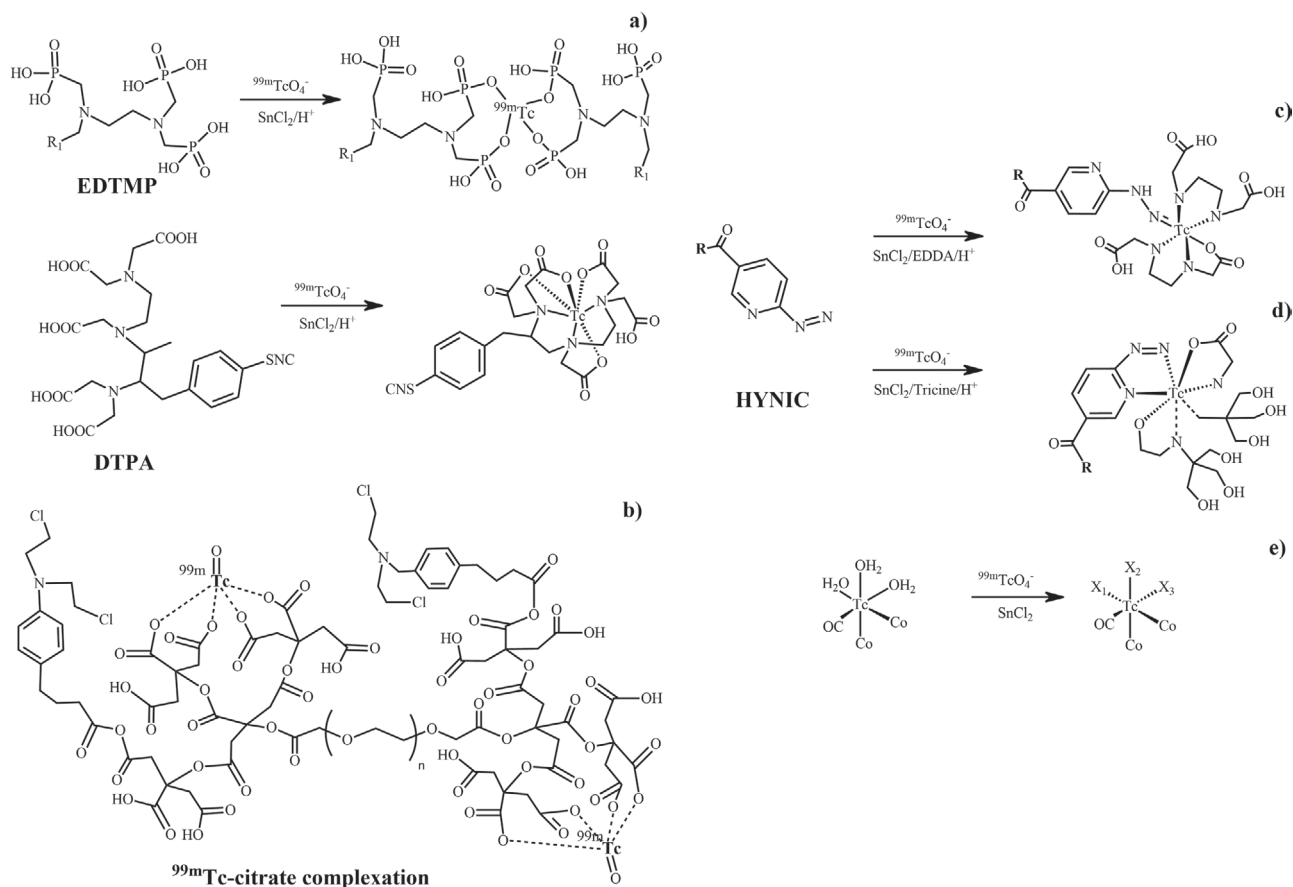


**Figure 2.** Common strategies for the  $^{99m}\text{Tc}$  radiolabeling of polymeric nanoparticles, where “R” represents a nanoparticle surface, using a) EDTMP, b) DTPA, c) EDDA/HYNIC, d) Tricine/HYNIC and e) direct radiolabeling.

diagnosis of FR-overexpressing tumors. The efficiency of the direct radiolabeling method was superior to 99% and stable up to 24 h. A significant cellular uptake and internalization of  $^{99m}\text{Tc}$ -CH/γ-PGA-FA NP was observed in HeDe cancer cells (+FR). The in vivo biodistribution of polymeric radiolabeled nanoparticles in adult male Fischer 344 rats (intravenous [iv]

administration) resulted in a rapid uptake by RES organs (liver, spleen, and bone marrow) and the accumulated radioactivity immediately started to wash out through the urinary tract (kidneys, urinary bladder, and urine). SPECT studies showed an uptake mediated by FR, and the authors concluded that  $^{99m}\text{Tc}$ -labeled folate nanoparticles had a higher selectivity and are able

**Table 1.** Micelles radiolabeled with  $^{99m}\text{Tc}$  and  $^{111}\text{In}$ .

Micelle			Radiolabeling			References
Composition	Preparation method	Size [nm]	Nuclide	Yield [%]	Strategies	
Peptide K237/FA-PEG-PLGA (K237: HTMYHHYQHHL)	W/O	115–143	$^{99m}\text{Tc}$	>97	Direct, with $\text{SnCl}_2$	[20]
0AcM-(PLA-PVA) (AcM: bevacizumab)	W/O/W	204–206		>90	Direct, with $\text{SnCl}_2$	[21]
EDTMP/PLA-PVA	W/O/W	200–500		>90	Direct, with $\text{SnCl}_2$	[22]
DTPA-(DSPE-PEG <sub>2000</sub> )	W/O/W	≈10		>90	Indirect, with DTPA	[23]
FA-(Chitosan-γ-PGA) (FA: folic acid)	Ionotropic gelation	75–200 average: 124		99	Direct, with $\text{SnCl}_2$	[24,26]
PLGA-Bendamustine	W/O/W	135–141		—	Direct, with $\text{SnCl}_2$	[25]
DTPA-PLGA	W/O	213.9		>90	Indirect, with DTPA	[28]
DTPA-PE/PGA y DTPA-PE/PGA-PEG	W/O/W	PGA:98-102 PGA-PEG: 111–121	$^{111}\text{In}$	≈50		[27]

to detect FR-overexpressing tumors with enhanced contrast. High-quality scans from a FR-overexpressing tumor (oral carcinoma) were also obtained.<sup>[24,26]</sup>

Khan et al. developed <sup>99m</sup>Tc-radiolabeled PLGA nanoparticles, loaded with bendamustine (BLPNP), as a delivery system for the effective targeting of leukemic cells. The radiolabeling strategy was carried out by the direct method, using stannous chloride. Nanoparticles with high radiochemical purity showed high uptake in liver, spleen, and kidney at 4-h after iv administration. Tumor accumulation was greater with regard to muscle at 1-h post-administration, confirming the passive accumulation within tumor via the EPR effect. Biodistribution studies also showed the in vivo stability of radiolabeled nanoparticle, demonstrating that PLGA nanoparticles were a suitable vehicle for drug transport and in vivo nanoparticle tracking (when radiolabeled).<sup>[25]</sup>

The biodistribution of radiolabeled polyglutamic acid (PGA)-based nanocapsules was reported. The radiolabeling was carried out using <sup>111</sup>In. In the study, PGA and PGA-PEG nanocapsules were compared. The <sup>111</sup>In radionuclide was incorporated using phosphoethanolamine, conjugated with the chelating agent DTPA (Figure 2a), which was entrapped within the hydrophobic core of the nanocapsules. The radiolabeling method offered a lower labeling yield (≈50%) and required a subsequent purification stage. The biodistribution of PGA and PGA-PEG nanocapsules indicated that both formulations have the capacity to reach the lymph nodes when administered by an iv or subcutaneous route. However, a liver accumulation was observed when nanoparticles were administered by the iv route. The data confirmed that nanocapsules are mainly excreted through the biliary and urinary routes. With the subcutaneous route, an enhancement in lymphatic uptake was observed, with regard to iv administration. The authors concluded that polyaminoacid nanocapsules exhibited properties useful for lympho-targeting applications.<sup>[27]</sup>

### 2.1.2. Dendrimers

The main radionuclide employed for dendrimer radiolabeling for imaging purposes is <sup>99m</sup>Tc (direct or indirect method; Figure 2) and, to a lesser extent, <sup>111</sup>In. The biodistribution of <sup>99m</sup>Tc-labeled dendrimers shows a similar pattern, regardless of the labeling method, though it varies depending on surface modifications and the route of administration.

Dendrimers usually accumulate in the liver and kidneys and are then excreted via the urinary,<sup>[29–33]</sup> or biliary route.<sup>[34]</sup> Glycodendrimers G-PPI [(poly(propyleneimine)-5.0G)-Mannose] and L-PPI [(poly(propyleneimine)-5.0G)-lactose] showed a significant difference in the rate of clearance. When dendrimers were carbohydrate-modified, the clearance from circulation was faster. The highest uptake was observed in the kidney (M-PPI) and liver/kidney (L-PPI), which indicates its fast excretion.<sup>[29]</sup>

A radiopharmaceutical based on the <sup>99m</sup>Tc-PEG-based dendrimer (G2), conjugated to chlorambucil, was reported. A change in biokinetic between free dendrimer and conjugated chlorambucil was evidenced, demonstrating that anionic globular PEG-based dendrimer significantly enhances the delivery of lipophilic drugs such as chlorambucil.<sup>[34]</sup>

Radiolabeled dendrimers via HYNIC, with different coligands (e.g., nicotinic acid, tricine, and ethylenediamine diacetic acid), have shown differences in blood and renal distribution, in agreement with the chemical nature of the coligand. All of them exhibit high accumulation in the liver (>30% of ID). The EDDA complex showed a significantly lower uptake in the spleen; urinary clearance showed that the radiolabeled conjugate was excreted unchanged or in a chemical form very similar to that initially injected. The authors concluded that radiolabeled PAMAM G4 dendrimers have great potential for imaging purposes.<sup>[30]</sup>

Tassano et al. reported the preparation and characterization of the fluorophore/technetium labeling of the PAMAM (G4) dendrimer as a potential molecular imaging agent. When biodistribution evaluations were carried out in C57BL/6 melanoma-bearing mice (B16-F1 cell line), as well as in normal mice, it was found that normal and tumor-bearing mice had similar behavior in renal and liver uptake; tumor uptake reached 9% ID after 3 h.<sup>[31]</sup>

A variety of dendrimer-folate conjugates (PAMAM 5G) were obtained by Zhan (2010) and Shan (2011),<sup>[32,33]</sup> which showed a rapid clearance from circulation in normal healthy mice (iv). Biodistribution was investigated with KB tumor-bearing nude mice. Agents remained at a low level, up to 6 h, in the FR-negative organs. Kidneys, which express FR, are the major clearance organs. For organs expressing FA receptors (liver, kidney, and tumor), their distribution experienced a significant increase in PEG-FA-dendrimer uptake. Micro-SPECT imaging confirmed predominant uptake of <sup>99m</sup>Tc-dendrimers-PEG-FA by the FR-positive tumors, concluding that radiolabeled <sup>99m</sup>Tc-G5-Ac-pegFA-DTPA is a promising imaging tool for cancer diagnosis.

Kojima et al. synthesized PEGylated lysine-bearing PAMAM dendrimers using different generations of the dendrimer, PEG lengths, and radiolabeled with <sup>111</sup>In using DTPA as the chelating agent (Figure 3). Biodistribution studies showed accumulation in the liver and kidneys after iv administration. Excretion of the acetylated dendrimer occurs via the kidneys, while the dendrimer conjugated to the peptide is excreted via the bile.<sup>[35]</sup> However, if administered subcutaneously, they remain in the tumor for an extended period of time and do not accumulate in other organs. The retention time in HPLC (molecular exclusion) correlates proportional to the molecular weight of the radiolabeled dendrimer. These results indicated that the subcutaneously-injected dendrimers might be used as drug depots around the injection site. Table 2 summarizes the radiolabeling strategies of dendrimers, represented in Figures 2 and 3.

## 2.2. Polymeric Nanoparticles Labeled with Positron-Emitting Radionuclides

PET-radiolabeled polymeric nanoparticles have satisfactory transport capacities, a well-defined geometry, and a well-known physicochemical behavior. The development of PET nanoprobes is susceptible to some restriction caused by the contradiction between intrinsic pharmacokinetics of NPs and the limited half-lives of positron-emitting radioisotopes. In an ideal pretargeted PET-imaging system, the tumor-targeting agents



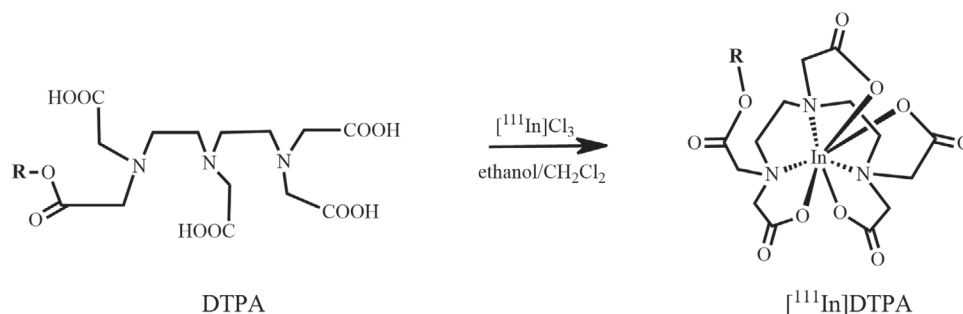


**Figure 3.** Radiolabeling strategy for the  $^{111}\text{In}$  radiolabeling of polymeric nanoparticles, using DTPA as a chelating agent, where “R” represents a nanoparticle surface.

should preferentially accumulate in tumors within a reasonable time frame and the uncombined radioligands should be rapidly cleared from the body to allow high-contrast tumor PET imaging.

A majority of the existing radiolabeled strategies with positron emitters use the anchorage of functional groups to surface nanoparticle as a first step. In the case of  $^{64}\text{Cu}$  or  $^{68}\text{Ga}$ , chelating agents such as 1,4,7,10-tetraazacyclododecane-1,4,7,10-tetraacetic acid (DOTA), 1,4,8,11-tetraazacyclotetradecane-1,4,8,11-tetraacetic acid (TETA), 1-(1-carboxy-3-carbo-*tert*-butoxypropyl)-4,7-(carbo-*tert*-butoxymethyl)-1,4,7-triazacyclononane (NODAGA), and 1,4,7-triazacyclononane-1,4,7-triacetic acid (NOTA), can be attached before (preradiolabeling) or after (post-radiolabeling) forming the nanoparticle. In the case of labeling with  $^{18}\text{F}$ , the chelation process is mainly carried out by halogenation reactions through

$-\text{C}-^{18}\text{F}$ ,  $-\text{B}-^{18}\text{F}$  and  $-\text{Si}-^{18}\text{F}$  or via chelation with  $\text{Al}-^{18}\text{F}$  complexes.<sup>[38]</sup> **Figure 4** summarizes the main  $^{18}\text{F}$ -labeling strategies. The clinical applications of PET-nanoparticles are still in an early stage and much more efforts are needed to obtain a

functional nanoparticle for PET imaging using fast radiolabeling strategies with high yields.

### 2.2.1. Polymeric Micelles

An efficient preparation procedure for  $^{18}\text{F}$ -radiolabeled polymeric micelles was described by Di Mauro and cols.<sup>[39]</sup> Polyester-based nanoparticles were prepared using a modified nano-coprecipitation method; the active radiolabeled agent 4- $^{18}\text{F}$ fluorobenzyl-2-bromoacetamide ( $^{18}\text{F}$ FBBA) was synthesized and condensed through three alternative methods, 1) with  $\alpha$ -thio- $\omega$ -carboxy poly (ethylene glycol), to form  $^{18}\text{F}$ -labeled PEG-thiol-acids, 2) with a product of the esterification reaction between 1,8-octanediol and glutaric acid, followed by the reaction with PEG 1500, and 3) the product of the microwave-assisted reaction to form a prepolymer based on glutaric acid and 1,8-octanediol at a molar ratio of 1:1.2. In order to acquire targeted NPs, a block copolymer attached via a linker to peptide AGBBB015F was used. The nanoparticles were prepared

**Table 2.**  $^{99\text{m}}\text{Tc}$  and  $^{111}\text{In}$ : radiolabeling strategies of dendrimers.

Dendrimer Structure	R/n	Radiolabeling		References
		Strategies	Radiochemical purity [%]	
PPI (5G)-Mannose	$^{99\text{m}}\text{Tc}$	Direct, with $\text{SnCl}_2$	>95	[29]
PPI (5G)-Lactose		Direct, with $\text{SnCl}_2$	>95	
PEG (2G)-Chlorambucil		Indirect, with citric acid	>95	[34]
PAMAM (4G)-HYNIC	$^{111}\text{In}$	Indirect, with coligand (nicotinic acid)	≈99	[30]
		Indirect, with coligand (EDDA)	≈99	
		Indirect, with coligand (tricine)	≈99	
PAMAM (4G)-TFIC		Direct, via $^{99\text{m}}\text{Tc}-(\text{CO})_3(\text{H}_2\text{O})_3^+$	>90	[31]
PAMAM (5G)-Ac-FA		Indirect, with DTPA	≈95	[32,33]
PAMAM(5G) Ac-peg-FA		Indirect, with DTPA	≈95	[32]
PAMAM (4G)-trastuzumab		Indirect, with DTPA	—	[36]
PAMAM (4G)-CP		Indirect, with DTPA	—	
PAMAM(G1)-DOTA and PAMAM (G4)-DOTA		Indirect, with DOTA	>95	[37]
PEG2k-Lys-PAMAM (G5), (G4) PEG5k-Lys-PAMAM (G4) Ac-Lys-PAMAM (G4)	Indirect, with Lys(DTPA)	—	[35]	

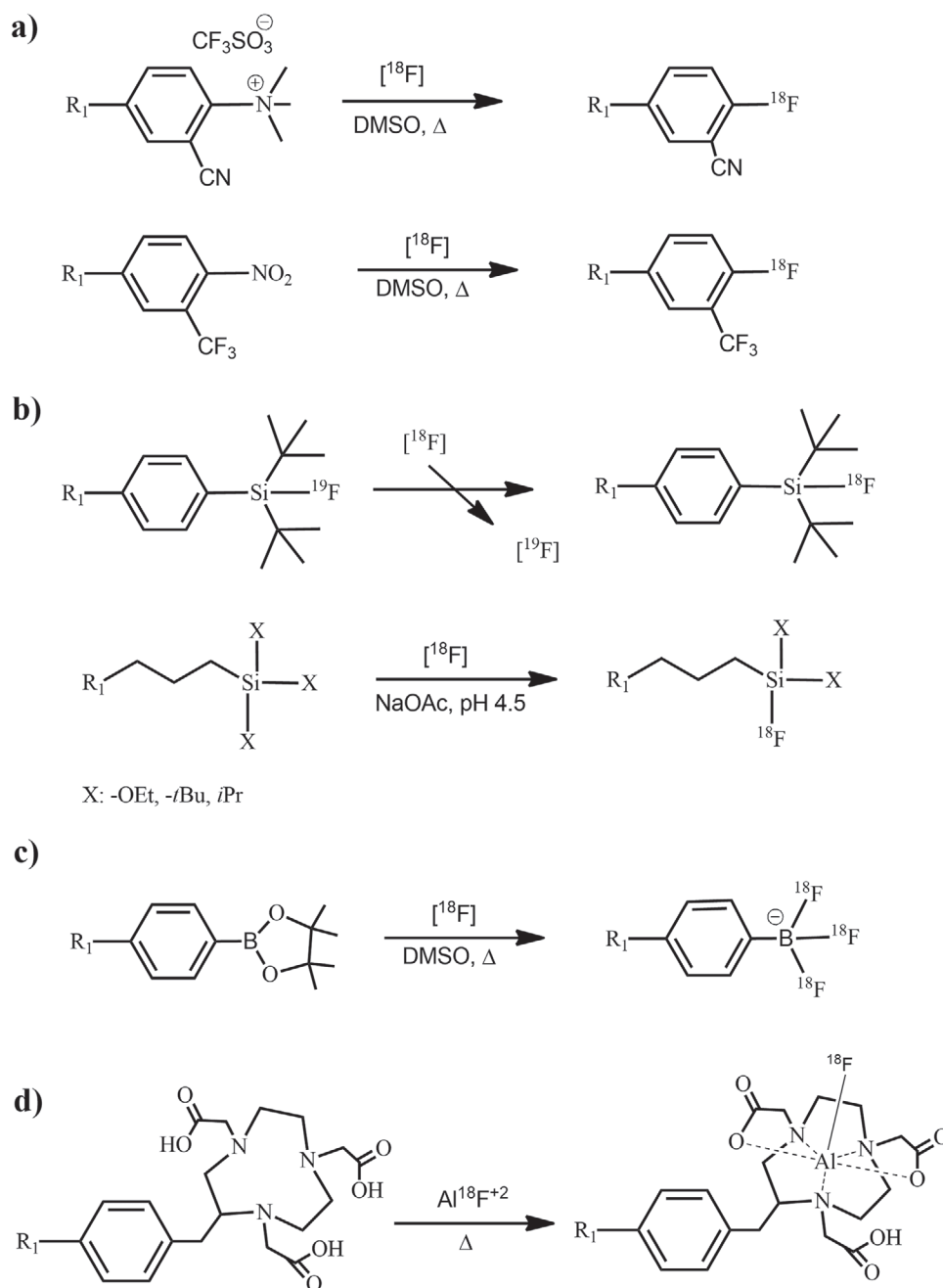


**Figure 4.** Radiolabeling strategies through a) C– $^{18}\text{F}$  bond formation, b) Si– $^{18}\text{F}$  bond formation, c) B– $^{18}\text{F}$  bond formation, and d) Al– $^{18}\text{F}$  chelation, where “R” represents a nanoparticle surface.

using a modified nano-coprecipitation method and were obtained with average diameters below 200 nm and narrow size distribution.

Berke et al.<sup>[40]</sup> preferred isotopic exchange. Nanoparticle preparation was carried out with controlled size in the sub-100 nm range by a microemulsion polymerization process using amphiphilic poly(2-oxazoline) block copolymers as polymer surfactants modified, with a silicon-fluoride-acceptor (SiFA: [4-(Bromomethyl)phenyl]di-*tert*-butylfluorosilane) and 1,6-hexanediol dimethacrylate (HDDMA, to swell the micellar core in water).

The nanoparticles were radiolabeled with fluorine-18 ( $^{18}\text{F}$ ), obtaining a highly stable –Si– $^{18}\text{F}$  derivate (Figure 4b). This labeling approach is an excellent alternative to chelator-functionalized nanoparticle systems where the chelator is attached to the post-NP formation. In vivo analysis, using a murine mammary tumor model (EMT6), revealed optimal tumor uptake driven by the EPR effect, with high tumor-to-muscle ratios for  $^{18}\text{F}$ -SiFA-NPs, with a size of  $\approx 33$  nm. These results are very promising for the development of NPs for functional molecular imaging and future NP-based targeted therapies.

Lee et al. have developed an efficient and straightforward method for radiolabeling glycol chitosan nanoparticles (CNPs) in order to determine its biodistribution. A simple strategy was reported for the preparation of  $^{64}\text{Cu}$ -radiolabeled via “click” chemistry, where a strain-promoted azide-alkyne cycloaddition technique is employed. Preparation of the glycol-chitosan polymeric core was carried out by a self-assembly method with posterior modification by 5 $\beta$ -cholanic acid, in order to obtain carboxylic-end nanoparticles. Posteriorly, polymeric cores were modified using a carbodiimide-type reaction with azide-PEG<sub>4</sub>-NHS, obtaining N<sub>3</sub>-CNPs. Authors synthesized the bifunctional chelator agent dibenzylcyclooctyne-PEG<sub>4</sub>-Lys-DOTA (DBCO-PEG<sub>4</sub>-Lys-DOTA) and complexed it with  $^{64}\text{Cu}$  for further conjugation with N<sub>3</sub>-CNPs, obtaining stable and radiochemically-pure (>98%) nanoparticles with a high specific activity. The quantitative analysis by micro-PET imaging demonstrated that  $^{64}\text{Cu}$ -CNPs was accumulated in tumor tissue with a prolonged circulation time in blood circulation, establishing a simple preradiolabeling approach to conveniently radiolabel nanoparticles for PET imaging.<sup>[41]</sup>

Using the same strategy, Lee et al.<sup>[41]</sup> designed chitosan-modified nanoparticles, which were conjugated to  $^{64}\text{Cu}$ -DOTA-Lys-PEG<sub>4</sub> and an activatable matrix metalloproteinase (MMP)-specific peptide probe (-Cy5.5), using a single-step bio-orthogonal “click” reaction (AMP-CNP-DOTA- $^{64}\text{Cu}$ ). Nanoparticles were characterized by DLS and spectrometric techniques. In vivo studies demonstrated a time-dependent tumor accumulation, with high uptake in liver and kidney and significant reduction of radioactivity in both organs after 48 h post-injection, which provides a good delimitation of the tumor region from surrounding tissues. *Ex vivo* near-infrared fluorescence (NIRF) molecular imaging was consistent with PET imaging, demonstrating the quantitative capability of dual  $^{64}\text{Cu}$ -CNP-Cy5.5 nanoparticles as a multimodal optical/PET image probe with possible clinical applications.<sup>[42]</sup>

Novel polymeric micelles for targeted atherosclerosis PET imaging were described by Woodard et al.<sup>[43]</sup> Polymeric cores were assembled from PEG-methacrylate, DOTA-methacrylate, and CANF-PEG-methacrylate, where natriuretic CANF peptide (98%, H-Arg-Ser-Ser-Cys-Phe-Gly-Gly-Arg-Ile-Asp-Arg-Ile-Gly-Ala-Cys-NH<sub>2</sub>) was used to target the natriuretic peptide receptors (NPRs) as potential targets for atherosclerosis imaging and therapy. The PET/CT imaging in a mouse apoE<sup>-/-</sup> model showed a higher net PET signal at atherosclerotic plaques, attributed to efficient binding to upregulated NPRs, located on atherosclerotic plaques, demonstrating a significant potential as a non-invasive approach for further evaluation of the progression of atherosclerosis.

### 2.2.2. Dendrimers

Dendrimers have been also explored as optional PET radiotracers using different PET emitter radionuclides such as  $^{18}\text{F}$ ,  $^{64}\text{Cu}$ ,  $^{68}\text{Ga}$ ,  $^{76}\text{Br}$ , and  $^{124}\text{I}$ . Trembleau et al. employed the B- $^{18}\text{F}$  link for the  $^{18}\text{F}$  labeling of a biotin-modified dendrimer (Figure 4c).<sup>[44]</sup> The radiolabeling was carried out using the conjugation of trifluoro-boroaryl moieties to the NH<sub>2</sub>-surface.

The development of a radiolabeling method for temperature-sensitive nanomaterials opened the field of chemistry for the conjugation of targeting molecules to improve the specificity of polymer-branched nanoparticles.<sup>[44,45]</sup> Additionally, Hou et al. prepared polymeric nanoparticles based on a self-assembly core of adamantane-grafted, first-generation polyamidoamine dendrimer (Ad-PAMAM),  $\beta$ -CD-grafted/TCO-branched polyethylenimine (TCO: bio-orthogonal reactive motif), and adamantane-functionalized PEG.<sup>[46]</sup>

The strategy for preparation was based on the high affinity between adamantane and cyclodextrines, giving way to the TCO-CNPs (50 nm) system. After iv injection of TCO-CNPs in tumor-bearing mice with subsequent accumulation via EPR effect, a small molecule containing both the complementary bio-orthogonal motif (tetrazine, Tz) and the positron-emitting radioisotope ( $^{64}\text{Cu}$ -DOTA-TZ) was injected to selectively and irreversibly react with TCO. The blood concentration of free  $^{64}\text{Cu}$ -Tz was less than 1% at 1.5 h. Compared to traditional nanoparticle-based imaging platforms, liver uptake was equivalent to tumor uptake, providing a robust and improved methodology for researchers and clinicians to pursue.<sup>[46,47]</sup> **Table 3** summarizes the main characteristics of some PET-radiolabeled devices based on dendrimer cores.

Bouziotis et al.<sup>[58]</sup> reported the hybrid radiolabeled nanoparticulate AGuIX-NPs system, based on polysiloxane cores surrounded by gadolinium chelates (DOTA( $\text{Gd}^{3+}$ )), as the first multifunctional silica-based NPs that are sufficiently small (<5 nm) to escape hepatic clearance and enable imaging by complementary techniques, including radiolabeling with  $^{111}\text{In}$  and  $^{68}\text{Ga}$ . Nanoparticles were prepared by using the top-down process and posteriorly functionalizing with the *N*-hydroxysuccinimide-(2,2'-(7-(1-carboxy-4-((2,5-dioxopyrrolidin-1-yl)oxy)-4-oxobutyl)-1,4,7-triazonane-1,4-diyl)diacetic acid) derivative (NODAGA-NHS) to form an amide bond. Afterward, nanoparticles were radiolabeled with  $^{68}\text{Ga}$ , obtaining a radiochemical purity greater than 99%. Serum stability studies showed no evidence of  $^{68}\text{Ga}$  (free or binding to protein) up to 3h. In vivo studies showed no degradation of  $^{68}\text{Ga}$ -AGuIX@NODAGA nanoparticles in mouse blood and urine samples at 60 min. These radiolabeled nanoparticles were rapidly cleared from the blood via the kidneys, causing extremely low background activity in all other tissues. A U87MG tumor-bearing mice model was used to determine tumor accumulation, finding a clear difference in the tumor/blood and tumor/muscle (T/M) ratios. Studies demonstrated the development of  $^{68}\text{Ga}$ -AGuIX@NODAGA nanoparticles, as a dual-modality imaging agent adequate for both PET and MR.

### 2.3. Polymeric Nanoparticles Radiolabeled as a Theranostic Approach

The basic requirement for theranostic applications is the suitable selection of a theranostic pair of radionuclides (beta or alpha emitters for therapy/gamma or positron emitters for imaging); however, a recently explored concept is the use of a single radionuclide for both imaging and therapy (Figure 5). In this sense, the most used theranostic radionuclides for labeling polymeric nanoparticles are  $^{131}\text{I}$  and  $^{177}\text{Lu}$ .



**Table 3.** Main characteristics of some PET-radiolabeled devices.

R/n	Dendritic core	Dendronizing molecules	Radiolabeling strategy	Ligand/Targeting	Reference	
<sup>64</sup> Cu	6-BAT(6-[p-(bromoacetamido)benzyl]-TETA)	LyP-1 c(CGNKRTRGC) or (ARALPSQRSR)	TETA	LyP-1 (CGNKTRTRGC)/p32 protein	[48]	
	PAMAM(G5.NH <sub>2</sub> )-Fluorescein isothiocyanate		DOTA	Folic acid/FR-expressing tumors	[49]	
	Pentaeritriol-	Polyglycerol-polysulfate	DMPTACN (1,4-bis(2-pyridinylmethyl)-1,4,7-triazacyclononane)	Multifunctional scaffold	[50]	
	PAMAM (G0.NH <sub>2</sub> )	Antibody, NIRF imaging probe (Cys5.5)	DOTA	HER-2 receptor	[51]	
<sup>68</sup> Ga	Polylysine-based dendrimer	N-glycan clusters	DOTA	In vivo dynamics and biodistributions between glycan-dendrimers	[52]	
		PAMAM (G4.NH <sub>2</sub> )	DOTA	Passive targeting to tumor tissue	[53]	
		PAMAM (NH <sub>2</sub> )	Hex-5-ynoic acid, bis-Boc-aminoxy acetic acid, and maleimido-hexanoic acid	DOTA	-RGD-/angiogenesis	[54]
		PAMAM	PEG	DOTA	—	[55]
		PAMAM	PEG	NODAGA	Pepsin/GRPr	[56]
<sup>76</sup> Br	Pentaerythritol	2,2-bis(hydroxymethyl)propanoic acid	Tyrosine moieties	-RGD-/angiogenesis	[57]	

### 2.3.1. Polymeric Micelles

The preparation of <sup>131</sup>I-labeled micelles based on mag-poly (HEMA–MAPA) by using the iodogen method has been reported.<sup>[59]</sup> The optimum radioiodination conditions and parameters were found to be at pH 9, 250 µg of iodogen, 1 mg

of the substrate, and 30 min at 37 °C (**Figure 6**). The labeling yield reported was about 95–100%, with high serum stability within 60 min, sufficient for imaging procedures. Biodistribution studies by scintigraphy showed notable uptake in the abdominal region, with a prevalence of the radiolabeled compound in organs such as lung, small intestine, spleen, and the uterus, as well as breast, ovary, and pancreas. The authors considered <sup>131</sup>I-mag-poly(HEMA–MAPA) as a diagnostic and therapeutic agent for the tumors in these organs.

The radiolabeling with <sup>177</sup>Lu is carried out using bifunctional chelating agents, such as DOTA and its analogs. This radiolabeling strategy is an efficient way to improve the complexation rate in polymeric nanoparticles. Recently, the preparation of radiolabeled (<sup>177</sup>Lu) PLGA nanoparticles (167 ± 57 nm) was described.<sup>[60]</sup> The PLGA core was modified with a hyaluronic acid shell and <sup>177</sup>Lu was chelated using the DOTA macrocycle,

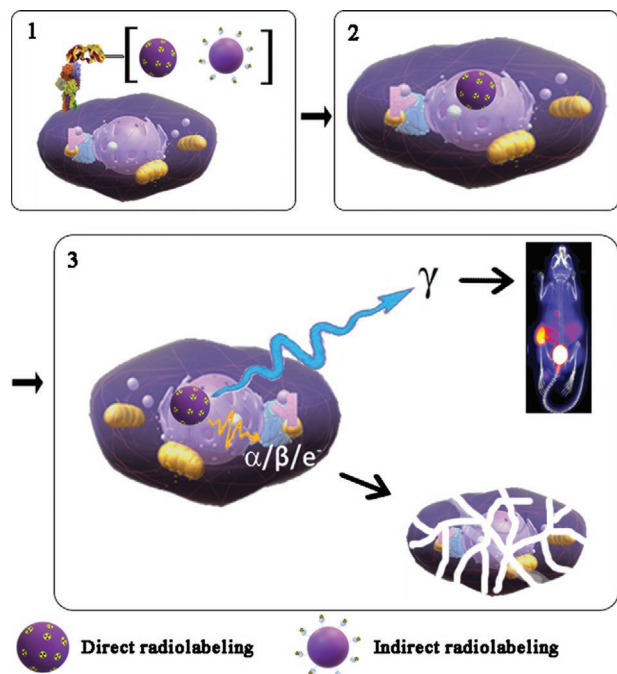
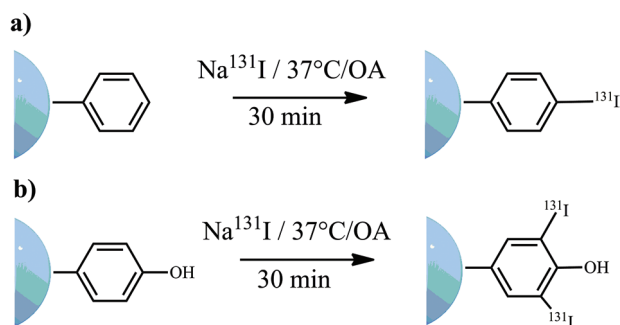


**Figure 5.** Representative scheme of the imaging and therapeutic effects of radiolabeled polymeric nanoparticles. 1) targeting to surface cell receptors, 2) Internalization or cellular uptake and 3) diagnostic, therapeutic or theranostic application, according to radioactive emission.



OA: Oxidizing agent, Choramine T, Iodogen

**Figure 6.** Typical iodination of polymeric nanoparticles using benzene-derivative moieties. Production of a) 4-Iodobencil and b) 2,6-diiodo-4-phenyl derivatives.

obtaining a therapeutic nanosystem based on bimodal mechanisms, chemotherapy using MTX as a disease-modifying antirheumatic drug, and the radionuclide as a radiotherapeutic component. Developed nanoparticles showed suitable properties for the radiosynovectomy and the disease monitoring molecular imaging as well as further specific targeted antirheumatic therapy.

The radiolabeled polymeric PLGA/paclitaxel (PLGA(PTX)) system conjugated to bombesin (Lys<sup>1</sup>-Lys<sup>3</sup>(DOTA)-BN) was recently reported. In this design, the DOTA molecule was employed as a linker site between the peptide and dendrimer surface (–NH<sub>2</sub>), and additional –CGG-DOTA was conjugated and radiolabeled to obtain <sup>177</sup>Lu-BN-PLGA(PTX). In vivo studies showed a significant accumulation in the tumor-bearing mouse model after 72 h. Therefore, these micelles are proposed as suitable strategies for bimodal breast cancer therapy due to the synergistic effect of <sup>177</sup>Lu and PTX, in addition it could be useful to record and monitor the disease progression by molecular imaging through the gamma emission.<sup>[61]</sup>

### 2.3.2. Dendrimers

The radiolabeling of PAMAM dendrimers with <sup>131</sup>I has been reported using the Chloramine T (Tosylchloramide sodium) method, using phenol groups previously conjugated (such as 3-(4'-hydroxyphenyl) propionic acid-OSu [HPAO]) to the dendrimer surface (Figure 7).<sup>[62,63]</sup>

In this way, a chlorotoxin-conjugated multifunctional dendrimer labeled with <sup>131</sup>I was prepared as a suitable platform, with the potential to be used for targeted SPECT imaging and radiotherapy of an MMP2-overexpressing glioma model. The NH<sub>2</sub>-PAMAM fifth-generation dendrimers (G5.NH<sub>2</sub>) were sequentially conjugated to PEG, targeting ligand chlorotoxin (CTX) and HPAO, followed by acetylation of the remaining terminal amines of dendrimers and radiolabeling with <sup>131</sup>I to form <sup>131</sup>I-G5.NHAc-HPAO-(PEG-CTX)-(mPEG), exhibiting good stability and cytocompatibility up to 20 μm. Targeting specificity for functional proteins like MMP2 and chloride ion channels (overexpressed in gliomas, medulloblastomas, prostate cancer, sarcomas, and intestinal cancer) proved to specifically target cancer cells overexpressing MMP2 via receptor-mediated binding and endocytosis. In vivo SPECT imaging also demonstrated specific targeting and higher tumor uptake. The biodistribution studies showed a significant accumulation in the liver, while the heart,

lung, tumor, kidney, spleen, intestines, stomach, and soft tissue had a relatively low accumulation of the nanoparticles. The authors demonstrated that the survival of tumor-bearing mice could be significantly prolonged after being treated with <sup>131</sup>I-G5.NHAc-HPAO-(PEG-CTX)-(mPEG) dendrimers. The <sup>131</sup>I-labeled multifunctional dendrimers may be used as a promising alternative for SPECT imaging and radiotherapy of different types of MMP2-overexpressing cancers.<sup>[62]</sup>

Cheng et al. reported multifunctional dendrimers radiolabeled with <sup>131</sup>I as a delivery system for both targeted therapy and imaging of gliomas. Polymeric cores were modified with *Buthus martensii* Karsch chlorotoxin (BmK CT), which selectively binds to tumors of neuroectodermal origin (including glioma cells) mediated by MMP-2 and annexin A2 on the cells. G5.NH<sub>2</sub>-mPEG dendrimers were synthesized and modified by the carbodiimide-type reaction with mPEG-COOH to obtain G5 mPEG dendrimers. Chlorotoxin was conjugated via maleimide-PEG. Finally, the radiolabeling was carried out to obtain the pure and stable <sup>131</sup>I-G5.NHAc-HPAO-(PEG-BmK CT)-(mPEG) system. Surface modifications demonstrate high levels of cytocompatibility with significant enhancement of the glioma targeting and radiotherapeutic effect using in vitro and in vivo models. The polymeric nanoparticulate system demonstrated potential applications for glioma-specific SPECT imaging and radiotherapy via iv administration.<sup>[63]</sup>

The most common strategies for dendrimer radiolabeling with <sup>177</sup>Lu is the use of bifunctional chelating agents such as DTPA, ethylenediaminetetraacetic acid, nitrilotriacetic acid, 1,4,7,10-tetraazacyclododecane-1,4,7-triacetic acid (DO3A), NOTA, and DOTA, which are previously conjugated to the dendrimer surface (via carbodiimide or HATU: 1-[Bis(dimethylamino)methylene]-1H-1,2,3-triazolo[4,5-b]pyridinium 3-oxide hexafluorophosphate), or using the most friendly reaction between DN-NH<sub>2</sub> with S-2-(4-isothiocyanatobenzyl)-1,4,7,10-tetraazacyclododecane acid (p-SCN-Bz-DOTA). The posterior radiolabeling is carried out in standard conditions with <sup>177</sup>LuCl<sub>3</sub>.

Biodistribution studies of <sup>177</sup>Lu-DOTA-PAMAM.G4 dendrimers prepared by Kovacs et al. in melanoma-bearing mice showed a high liver and splenic uptake and rapid renal clearance. Additional alteration in element concentrations in tumor tissues was observed, probably due to the effect of radiation in tissues.<sup>[64]</sup>

Multifunctional imaging and therapy nanoprobe, based on radiolabeled <sup>177</sup>Lu-dendrimer (PAMAM(G4)NH<sub>2</sub>) and conjugated to folate and bombesin with gold nanoparticles in the dendritic cavity (<sup>177</sup>Lu-Den-AuNP-folate-bombesin) allows the integration of fluorescent and plasmonic-photothermal properties.<sup>[65,66]</sup> Targeting moieties (FA and bombesin) were attached to amides via the HATU reaction. Gold nanoparticles were introduced into the PAMAM cavity by in situ reductions of HAuCl<sub>4</sub> using NaBH<sub>4</sub>. In vitro studies demonstrated the potential of the targeted radiotherapeutic <sup>177</sup>Lu-Den-AuNP-folate-bombesin. It was about four times more lethal than <sup>177</sup>Lu-Den-AuNP. The authors conclude that the radiolabeled and functionalized Den-AuNP has the ability for internalization into cancer cells and exhibits suitable properties for optical imaging, plasmonic-photothermal therapy, and targeted radiotherapy.

<sup>177</sup>Lu-labeled PAMAM dendrimer (DN), loaded with PTX and functionalized with Lys<sup>1</sup>Lys<sup>3</sup>(DOTA)-bombesin (BN) peptide for specific targeting of gastrin-releasing peptide receptors (GRPr)

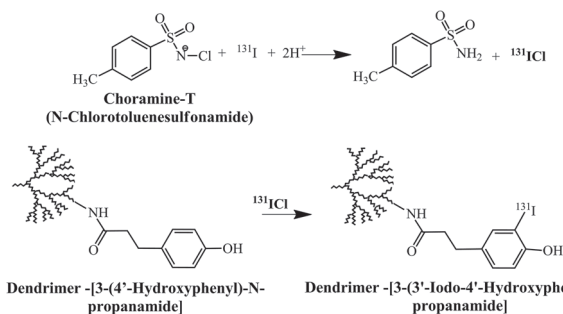


**Figure 7.** Strategy for PAMAM dendrimer <sup>131</sup>I radiolabeling using HPAO as a chelating agent.

overexpressed on breast cancer cells, merges chemotherapy (PTX) and radiotherapy ( $^{177}\text{Lu}$ ). The result of combining  $^{177}\text{Lu}$  with PTX was a very considerable reduction in the viability of T47D cells treated with  $^{177}\text{Lu}$ -DOTA-DN(PTX)-BN. The radiopharmaceutical showed suitable characteristics for targeted therapy applications in GRPr-positive tumors.<sup>[67]</sup>

The evaluation of the first (G1-) or fourth (G4-) generation PAMAM dendrimer conjugates with the DOTA-like bifunctional chelator (2-methyl) pyridine-*N*-oxide pendant arm (DO3A-py<sup>NO-C</sup>), was reported by Laznickova et al. The radiolabeled dendrimers [ $^{177}\text{Lu}$ (G1-PAMAM-DO3A-py<sup>NO-C</sup>)] and [ $^{177}\text{Lu}$ (G4-PAMAM-DO3A-py<sup>NO-C</sup>)] were obtained with good stability, high specific activity, and radiochemical purity. Biodistribution studies in rats were carried out to elucidate the fate of radiolabeled dendrimers; G1-dendrimer administration was preferable, compared to the G4-dendrimer, due to its fast elimination and non-specific radioactivity uptake. Both complexes exhibited a rapid elimination from blood with renal and hepatic clearance. Results indicate that the employment of radiolabeled dendrimers might represent a prospective method for radiolabeling antibodies or their fragments with high specific activity and desirable biologic behavior.<sup>[68]</sup>

### 3. Conclusion

Polymer-based nano-radiopharmaceuticals offer promising alternatives as diagnostic, therapeutic, or theranostic tools. The diversity in core materials, surface modification, targeting strategies, radionuclides, etc., offers multiple possibilities for preparing multifunctional platforms for multimodal imaging (SPECT, PET, and CT) and therapy (chemotherapy and radiotherapy). However, the effective design of multimodal nanomedicines requires new radiochemical methods to overcome the limitations imposed by the conventional prosthetic groups and chelate-based chemistries. It is necessary to develop new and fast methods of labeling, especially for radionuclides of a very short half-life. Chelate-free methods exploit the intrinsic chemical properties of nanoparticles to carry out simple and efficient radiolabeling.

### Acknowledgements

This study was partially supported by the National Council of Science and Technology (CONACyT-CB-A1-S38087) and the International Atomic Energy Agency (CRP-F22064, Contract 18358). It was carried out as part of the activities of the “Laboratorio Nacional de Investigación y Desarrollo de Radiofármacos”, CONACyT.

### Conflict of Interest

The authors declare no conflict of interest.

### Author Contributions

K.I.-O. and B.E.O.G. analyzed the information about polymeric nanoparticles labeled with gamma-emitting radionuclides (SPECT).

L.M.-A. and G.F.-F. analyzed the information about polymeric nanoparticles labeled with a positron-emitting radionuclide (PET). E.M.-A. and L.A.-L. collected and analyzed information of the labeled techniques, design, and drawing of figures, and were a major contributor in writing the manuscript. All authors read and approved the final manuscript.

### Keywords

nanomedicines, nuclear imaging, polymeric nanoparticles, radiolabeling strategies, theranostic applications

Received: October 16, 2020

Revised: December 2, 2020

Published online:

- [1] S. Bhatia, *Natural Polymer Drug Delivery Systems*, Springer International Publishing, Cham, Switzerland **2016**, pp. 33–93.
- [2] M. A. Kamal, N. Jabir NR, A. Tabrez, D. Shakil, *Int. J. Nanomed.* **2012**, *7*, 4391.
- [3] L. Jaimes-Aguirre, B. Vianey Gibbens-Bandala, E. Morales-Avila, B. Eli Ocampo-García, M. Seyedeh-Fatemeh, A. Amirhosein, *Curr. Pharm. Des.* **2016**, *22*, 2886.
- [4] S. Tinkle, S. E. Mcneil, S. Mühlebach, R. Bawa, G. Borchard, Y. C. Barenholz, L. Tamarkin, N. Desai, *Ann. N. Y. Acad. Sci.* **2014**, *1313*, 35.
- [5] H. M. N. Iqbal, A. M. V. Rodriguez, R. Khandia, A. Munjal, K. Dhama, *Recent Pat. Inflammation Allergy Drug Discovery* **2017**, *10*, 86.
- [6] D. Bobo, K. J. Robinson, J. Islam, K. J. Thurecht, S. R. Corrie, *Pharm. Res.* **2016**, *33*, 2373.
- [7] B. Fortuni, T. Inose, M. Ricci, Y. Fujita, I. Van Zundert, A. Masuhara, E. Fron, H. Mizuno, L. Latterini, S. Rocha, H. Uji-i, *Sci. Rep.* **2019**, *9*, 2666.
- [8] D. Rosenblum, N. Joshi, W. Tao, J. M. Karp, D. Peer, *Nat. Commun.* **2018**, *9*, 1410.
- [9] R. van der Meel, E. Sulheim, Y. Shi, F. Kiessling, W. J. M. Mulder, T. Lammers, *Nat. Nanotechnol.* **2019**, *14*, 1007.
- [10] M. Prasad, U. P. Lambe, B. Brar, I. Shah, M. J. K. Ranjan, R. Rao, S. Kumar, S. Mahant, S. K. Khurana, H. M. N. Iqbal, K. Dhama, J. Misri, G. Prasad, *Biomed. Pharmacother.* **2018**, *97*, 1521.
- [11] D. Lombardo, M. A. Kiselev, M. T. Caccamo, *J. Nanomater.* **2019**, *2019*, 3702518.
- [12] A. P. Singh, A. Biswas, A. Shukla, P. Maiti, *Signal Transduction Targeted Ther.* **2019**, *4*, 33.
- [13] E. Abbasi, S. Aval, A. Akbarzadeh, M. Milani, H. Nasrabadi, S. Joo, Y. Hanifehpour, K. Nejati-Koshki, R. Pashaei-Asl, *Nanoscale Res. Lett.* **2014**, *9*, 247.
- [14] R. Araújo, S. Santos, E. Igne Ferreira, J. Giarolla, *Molecules* **2018**, *23*, 2849.
- [15] S. Hossen, M. K. Hossain, M. K. Basher, M. N. H. Mia, M. T. Rahman, M. J. Uddin, *J. Adv. Res.* **2019**, *15*, 1.
- [16] S. Shen, Y. Wu, Y. Liu, D. Wu, *Int. J. Nanomed.* **2017**, *12*, 4085.
- [17] C. Cao, J. Zhao, M. Lu, C. J. Garvey, M. H. Stenzel, *Biomacromolecules* **2019**, *20*, 1545.
- [18] National Research Council (US) and Institute of Medicine (US) Committee on State of the Science of Nuclear Medicine, *Advancing Nuclear Medicine Through Innovation*, National Academies Press, Washington, DC **2007**.
- [19] G. Ferro-Flores, B. E. Ocampo-García, C. L. Santos-Cuevas, E. Morales-Avila, E. Azorín-Vega, *Curr. Med. Chem.* **2014**, *21*, 124.
- [20] Z. He, X. Zhang, J. Huang, Y. Wu, X. Huang, J. Chen, J. Xia, H. Jiang, J. Ma, J. Wu, *Oncotarget* **2016**, *7*, 76635.



- [21] T. B. Ligiero, C. Cerqueira-Coutinho, M. de Souza Albarnaz, M. Szwed, E. S. Bernardes, M. A. V. Wasserman, R. Santos-Oliveira, *Biomed. Phys. Eng. Express* **2016**, *2*, 04501.
- [22] B. F. C. de Patrício, M. S. de Albarnaz, M. A. Sarcinelli, S. M. de Carvalho, R. Santos-Oliveira, G. Weissmüller, *J. Biomed. Nanotechnol.* **2014**, *10*, 1242.
- [23] C. M. R. Oda, R. S. Fernandes, S. C. de Araújo Lopes, M. C. de Oliveira, V. N. Cardoso, D. M. Santos, A. M. de Castro Pimenta, A. Malachias, R. Paniago, D. M. Townsend, P. M. Colletti, D. Rubello, R. J. Alves, A. L. B. de Barros, E. A. Leite, *Biomed. Pharmacother.* **2017**, *89*, 268.
- [24] A. Polyák, I. Hajdu, M. Bodnár, G. Trencsényi, Z. Pöstényi, V. Haász, G. Jánoki, G. A. Jánoki, L. Balogh, J. Borbély, *Int. J. Pharm.* **2013**, *449*, 10.
- [25] I. Khan, A. Gothwal, A. Kaul, R. Mathur, A. K. Mishra, U. Gupta, *Pharm. Res.* **2018**, *35*, 200.
- [26] A. Polyák, I. Hajdu, M. Bodnár, G. Dabasi, R. P. Jóba, J. Borbély, L. Balogh, *Int. J. Pharm.* **2014**, *474*, 91.
- [27] R. Abellan-Pose, M. Rodríguez-Évora, S. Vicente, N. Csaba, C. Évora, M. J. Alonso, A. Delgado, *Eur. J. Pharm. Biopharm.* **2017**, *112*, 155.
- [28] S. Subramanian, U. Pandey, D. Gugulothu, V. Patravale, G. Samuel, *Cancer Biother. Radiopharm.* **2013**, *28*, 598.
- [29] H. B. Agashe, A. K. Babbar, S. Jain, R. K. Sharma, A. K. Mishra, A. Asthana, M. Garg, T. Dutta, N. K. Jain, *Nanomedicine* **2007**, *3*, 120.
- [30] L. Kovacs, M. Tassano, M. Cabrera, M. Fernández, W. Porcal, R. M. Anjos, P. Cabral, *Curr. Radiopharm.* **2014**, *7*, 115.
- [31] M. R. Tassano, P. F. Audicio, J. P. Gambini, M. Fernandez, J. P. Damian, M. Moreno, J. A. Chabalgoity, O. Alonso, J. C. Benech, P. Cabral, *Bioorg. Med. Chem. Lett.* **2011**, *21*, 5598.
- [32] Y. Zhang, Y. Sun, X. Xu, X. Zhang, H. Zhu, L. Huang, Y. Qi, Y. M. Shen, *J. Med. Chem.* **2010**, *53*, 3262.
- [33] L. Shan, *Molecular Imaging and Contrast Agent Database (MICAD)*, National Center for Biotechnology Information Bethesda USA **2011**.
- [34] S. Ghoreishi, A. Khalaj, A. Bitarafan-Rajabi, A. Azar, M. Ardestani, A. Assadi, *Drug. Res.* **2016**, *67*, 149.
- [35] C. Kojima, C. Regino, Y. Umeda, H. Kobayashi, K. Kono, *Int. J. Pharm.* **2010**, *383*, 293.
- [36] C. Chan, Z. Cai, R. M. Reilly, *Pharm. Res.* **2013**, *30*, 1999.
- [37] V. Biricová, A. Lázníčková, M. Lázníček, M. Poláček, P. Hermann, *J. Pharm. Biomed. Anal.* **2011**, *56*, 505.
- [38] H. S. Krishnan, L. Ma, N. Vasdev, S. H. Liang, *Chem. - Eur. J.* **2017**, *23*, 15553.
- [39] P. P. Di Mauro, V. Gómez-Vallejo, Z. B. Maldonado, J. L. Roig, S. Borrós, *Bioconjugate Chem.* **2015**, *26*, 582.
- [40] S. Berke, A.-L. Kampmann, M. Wuest, J. J. Bailey, B. Glowacki, F. Wuest, K. Jurkschat, R. Weberskirch, R. Schirrmacher, *Bioconjugate Chem.* **2018**, *29*, 89.
- [41] D.-E. Lee, J. H. Na, S. Lee, C. M. Kang, H. H. N. Kim, S. J. Han, H. Kim, Y. S. Choe, K.-H. Jung, K. C. Lee, K. Choi, I. C. Kwon, S. Y. Jeong, K.-H. Lee, K. Kim, *Mol. Pharmaceutics* **2013**, *10*, 2190.
- [42] S. Lee, S.-W. Kang, J. H. Ryu, J. H. Na, D.-E. Lee, S. J. Han, C. M. Kang, Y. S. Choe, K. C. Lee, J. F. Leary, K. Choi, K.-H. Lee, K. Kim, *Bioconjugate Chem.* **2014**, *25*, 601.
- [43] P. K. Woodard, Y. Liu, E. D. Pressly, H. P. Luehmann, L. Detering, D. E. Sultan, R. Laforest, A. J. McGrath, R. J. Gropler, C. J. Hawker, *Pharm. Res.* **2016**, *33*, 2400.
- [44] L. Trembleau, M. Simpson, R. W. Cheyne, I. Escofet, M. Appleyard, K. Murray, S. Sharp, A. M. Thompson, T. A. D. Smith, *New J. Chem.* **2011**, *35*, 2496.
- [45] L. Zhao, X. Shi, J. Zhao, *Drug Delivery* **2017**, *24*, 81.
- [46] S. Hou, J. Choi, M. A. Garcia, Y. Xing, K. K.-J. Chen, Y.-M. Chen, T. Ro, L. Wu, D. B. Stout, J. S. Tomlinson, H. Wang, K. Chen, H.-R. Tseng, W.-Y. Li, *ACS Nano* **2016**, *10*, 1417.
- [47] H. Wang, S. Wang, H. Su, K.-J. Chen, A. L. Armijo, W.-Y. Lin, Y. Wang, J. Sun, K.-i. Kamei, J. Czernin, C. G. Radu, H.-R. Tseng, *Angew. Chem., Int. Ed.* **2009**, *48*, 4344.
- [48] J. W. Seo, H. Baek, L. M. Mahakian, J. Kusunose, J. Hamzah, E. Ruoslahti, K. W. Ferrara, *Bioconjugate Chem.* **2014**, *25*, 231.
- [49] W. Ma, F. Fu, J. Zhu, R. Huang, Y. Zhu, Z. Liu, J. Wang, P. S. Conti, X. Shi, K. Chen, *Nanoscale* **2018**, *10*, 6113.
- [50] K. Pant, D. Gröger, R. Bergmann, J. Pietzsch, J. Steinbach, B. Graham, L. Spiccia, F. Berthon, B. Czarny, L. Devel, V. Dive, H. Sthepan, R. Haag, *Bioconjugate Chem.* **2015**, *26*, 906.
- [51] Y. Wang, Z. Miao, G. Ren, Y. Xu, Z. Cheng, *Chem. Commun.* **2014**, *50*, 12832.
- [52] K. Tanaka, E. R. O. Siwu, K. Minami, K. Hasegawa, S. Nozaki, Y. Kanayama, K. Koyama, W. C. Chen, J. C. Paulson, Y. Watanabe, K. Fukase, *Angew. Chem., Int. Ed.* **2010**, *49*, 8195.
- [53] A. Ghai, B. Singh, P. Panwar Hazari, M. K. Schultz, A. Parmar, P. Kumar, S. Sharma, D. Dhawan, A. K. Mishra, *Appl. Radiat. Isot.* **2015**, *105*, 40.
- [54] C. Wängler, S. Maschauer, O. Prante, M. Schäfer, R. Schirrmacher, P. Bartenstein, M. Eisenhut, B. Wängler, *ChemBioChem* **2010**, *11*, 2168.
- [55] G. Fischer, B. Wängler, C. Wängler, *Molecules* **2014**, *19*, 6952.
- [56] S. Lindner, C. Michler, B. Wängler, P. Bartenstein, G. Fischer, R. Schirrmacher, C. Wängler, *Bioconjugate Chem.* **2014**, *25*, 489.
- [57] A. Almutairi, R. Rossin, M. Shokeen, A. Hagooley, A. Ananth, B. Capocchia, S. Guillaudeu, D. Abendschein, C. J. Anderson, M. J. Welch, J. M. J. Fréchet, *Proc. Natl. Acad. Sci. U. S. A.* **2009**, *106*, 685.
- [58] P. Bouziotis, D. Stellas, E. Thomas, C. Truillet, C. Tsoukalas, F. Lux, T. Tsotakos, S. Xanthopoulos, M. Paravatou-Petsotas, A. Gaitanis, L. A. Mouloupoulos, V. Koutoulidis, C. D. Anagnostopoulos, O. Tillement, *Nanomedicine* **2017**, *12*, 1561.
- [59] U. Avcıbaşı, H. Demiroğlu, M. Ediz, H. A. Akalin, E. Özçalışkan, H. Şenay, C. Türkcın, Y. Özcan, S. Akgöl, N. Avcıbaşı, *J. Labelled Compd. Radiopharm.* **2013**, *56*, 708.
- [60] R. M. Trujillo-Nolasco, E. Morales-Avila, B. E. Ocampo-García, G. Ferro-Flores, B. V. Gibbens-Bandala, A. Escudero-Castellanos, K. Isaac-Olive, *Mater. Sci. Eng., C* **2019**, *103*, 109766.
- [61] B. Gibbens-Bandala, E. Morales-Avila, G. Ferro-Flores, C. Santos-Cuevas, L. Meléndez-Alafrot, M. Trujillo-Nolasco, B. E. Ocampo-García, *Mater. Sci. Eng., C* **2019**, *105*, 110043.
- [62] L. Zhao, J. Zhu, Y. Cheng, Z. Xiong, Y. Tang, L. Guo, X. Shi, J. Zhao, *ACS Appl. Mater. Interfaces* **2015**, *7*, 19798.
- [63] Y. Cheng, J. Zhu, L. Zhao, Z. Xiong, Y. Tang, C. Liu, L. Guo, W. Qiao, X. Shi, J. Zhao, *Nanomedicine* **2016**, *11*, 1253.
- [64] L. Kovacs, M. Tassano, M. Cabrera, C. B. Zamboni, M. Fernández, R. M. Anjos, P. Cabral, *Cancer Biother. Radiopharm.* **2015**, *30*, 405.
- [65] H. Mendoza-Nava, G. Ferro-Flores, F. D. M. Ramírez, B. Ocampo-García, C. Santos-Cuevas, L. Aranda-Lara, E. Azorín-Vega, E. Morales-Avila, K. Isaac-Olivé, *J. Nanomater.* **2016**, *2016*, 1039258.
- [66] H. Mendoza-Nava, G. Ferro-Flores, M. RamírezFde, B. Ocampo-García, C. Santos-Cuevas, E. Azorín-Vega, N. Jiménez-Mancilla, M. Luna-Gutiérrez, K. Isaac-Olivé, *Mol. Imaging* **2017**, *16*, 1536012117704768.
- [67] B. Gibbens-Bandala, E. Morales-Avila, G. Ferro-Flores, C. Santos-Cuevas, M. Luna-Gutiérrez, G. Ramírez-Nava, B. Ocampo-García, *Polymers* **2019**, *11*, 1572.
- [68] A. Laznickova, V. Biricova, M. Laznickec, P. Hermann, *Appl. Radiat. Isot.* **2014**, *84*, 70.



**Liliana Aranda-Lara** is professor of medical physics at the Universidad Autónoma del Estado de México. She was awarded a Ph.D. in health sciences and she has worked as a researcher since 2017. Her research interests include broad fields of radiobiology, nuclear medicine, molecular imaging, radiopharmacy, nano-radiopharmaceuticals, nanomedicine, and cancer chemoradiotherapy.